Available online at www.sciencedirect.com

ScienceDirect

IFAC PapersOnLine 56-2 (2023) 3146–3151

Two-layer Coalitional Model Predictive Control for Parabolic-Trough Collector Fields ⋆

A. Sánchez-Amores *, **J. M. Maestre** *, **E. F. Camacho** *

* *Systems and Automation Engineering Department, University of Seville, Spain (e-mail: {asamores,pepemaestre,efcamacho}@us.es).*

Abstract: Coalitional control partitions a system into multiple clusters or coalitions that solve independent local subproblems in parallel. This paper presents a two-layer coalitional model predictive control approach for regulation in constrained-coupled subsystems. We formulate a resource allocation mechanism to distribute the coupled constraint so that the global control problem can be solved in a decentralized manner, guaranteeing the satisfaction of the common constraint. In particular, a top layer will calculate the system's partition according to a given criterion and supervise the shared resource allocation. In turn, the lower control layer will calculate the local optimization problems for every coalition in a decentralized fashion, according to the available shared resource determined by the upper layer. This strategy is applied to regulate the outlet temperature of parabolic-trough solar collector fields, which are composed of a set of loops that remain coupled through a global shared resource constraint.

Keywords: Model predictive control, coalitional control, decentralized control, distributed solar collector field, resource allocation, decoupling problems.

1. INTRODUCTION

Over the last few decades, there has been a growing awareness of the harmful impact of fossil fuels on the environment and, consequently, on our welfare. As a result, there is great interest in promoting the development of alternative and clean energy sources. Renewable energy comes from natural sources such as the sun, wind, or water. They are non-polluting since they generate almost zero greenhouse gas emissions, reduce the carbon footprint, and, unlike non-renewable sources, they do not produce waste. In particular, solar energy is the most abundant source of energy on Earth (Kabir et al. (2018)), and can be exploited by using photovoltaic (PV) cells and concentrating solar power (CSP) systems. While PV cells directly use solar energy to generate electricity (Rathore et al. (2021)), CSP systems concentrate solar radiation, heating a fluid to produce steam, driving a turbine that will provide electrical power. Among all the types of technologies that comprise CSP systems (Islam et al. (2018); Zhang et al. (2013)), this paper focuses on parabolic-trough solar collector fields (Camacho et al. (2007)).

The main difference between solar plants with respect to other power processes is that the solar energy cannot be manipulated and therefore acts as an exogenous disturbance for the system that changes on a seasonal and daily basis. Among the different control frameworks available, model predictive control (MPC) can deal with constraints, disturbances, and delays, through a continuous replanning strategy following a receding-horizon approach. For example, Vasallo and Bravo (2016) formulate an MPC approach for optimal scheduling in CSP plants. Also, Alsharkawi and Rossiter (2016) estimate a linear model and apply a dual MPC for tracking and disturbance rejection.

However, solar fields are large-scale systems, leading to a high computational burden due to their high number of optimization variables. Thus, solving the optimization problem in a centralized manner can be computationally demanding for the available processing times. Coalitional control (Baldivieso-Monasterios and Trodden (2021); Fele et al. (2017)) satisfies the requirements of large-scale systems, partitioning the system into loosely coupled clusters of local controllers, achieving a trade-off between coordination and performance. Nevertheless, the collectors in parabolic-trough solar plants have a shared resource, which couples these subsystems through a common constraint that makes the partitioning of the global control problem challenging, as we seek to satisfy the constraint in a decentralized manner.

This paper proposes a two-layer coalitional MPC algorithm for parabolic-trough collector fields, in which the top layer is responsible for distributing the shared resource corresponding to the coupled constraint based on the requirements of the subsystems. In addition, coalitions will solve their local control problems in the bottom layer subject to the resource allocation provided. Also, coalitions may share their excess in the common resource or request if they need more than what has been supplied. This type of coalitional resource sharing problem has been addressed in continuous time by Barreiro-Gomez et al. (2015). Also, a

⋆ This work has received funding from the European Research Council (ERC) under the European Union's Horizon 2020 research and innovation program (OCONTSOLAR, grant agreement No 789051), and project C3PO-R2D2 (Grant PID2020-119476RB-I00 funded by MCIN/AEI/ 10.13039/501100011033).

10.1016/j.ifacol.2023.10.1448

hierarchical MPC for electricity networks that dynamically partitions a set of generators, storage systems, and loads into locally controlled clusters is presented by La Bella et al. (2021). If the local sources are not enough to balance the cluster's load changes, the supervisory layer distributes extra resources available from the other clusters. More recently, Masero et al. (2022) proposed a market where collectors could trade flow so as to maximize the performance of a solar plant using a coalitional strategy. Unlike these works, here collectors are grouped in coalitions based on their received irradiance. Then, a virtual state is used to collect the exceeding heating transfer flow so it can be redistributed to other coalitions.

The rest of the paper is organized as follows. Section 2 describes the concentrated-parameter model and operational constraints of the parabolic-trough solar collector field. In Section 3, we present the control objective and motivate the need for a resource allocation mechanism to solve the global problem in a decentralized fashion. Furthermore, the basic setting for coalitional control and the proposed algorithm is introduced. Section 4 provides simulation results on a 100 loop solar collector field, and concluding remarks are given in Section 5.

2. PARABOLIC-TROUGH PLANT MODEL

This section presents the characteristics of the ACUREX parabolic-trough solar collector field (Camacho et al. (1997)), located in *Plataforma Solar de Almería*, Spain. We can describe the field as a set $\mathcal{L} = \{1, \dots, N\}$ of N parallel loops, where each loop is formed by four 12-module collectors connected in series. The collectors are a set of curved mirrors that concentrate the solar direct normal irradiance (DNI) onto a receiver pipe. A heat transfer fluid (HTF) heats up as it flows along the pipe, transporting thermal energy to feed a steam turbine and generate electrical energy. In this case, Therminol 55 is used as HTF, and its density (ρ_f) and specific heat capacity (c_f) depend on the temperature of the fluid (T_f) as follows:

$$\rho_f(T_f) = 903 - 0.672T_f,\ c_f(T_f) = 1820 + 3.478T_f. \quad (1)$$

2.1 Concentrated parameter model of a loop

The concentrated parameter model provides a lumped description of each loop $j \in \mathcal{L}$ through the variation in the internal energy of the fluid. Consequently, the dynamics of the outlet temperature of a loop T_j can be described as

$$C_j \frac{dT_j}{dt} = \alpha_j \eta S I - \beta_j S H_j \left(\bar{T}_j - T^a\right) - q_j P_j (T_j - T_j^{in}), \quad (2)$$

$\forall j \in \mathcal{L}$, with $C_j = \rho_f(T_j)\, c_f(T_j)\, a_f L$, $P_j = \rho_f(T_j)\, c_f(T_j)$, and $\bar{T}_j = 0.5\left(T_j + T_j^{in}\right)$.

To capture the differences in loops dynamics, we have introduced two scale factors $\{\alpha_j, \beta_j\}$ to characterize the cleanliness of the collectors and the thermal losses of each loop, respectively. Furthermore, the global coefficient of thermal losses H_j depends on the mean inlet-outlet temperature of the loop and on the ambient temperature, and its expression can be found in Carmona (1985). Note that the properties of the HTF defined in (1) become dependent on the outlet temperature of the loop T_j. Model variables and parameters are summarized in Table 1.

Table 1. Variables and model parameters

Symbol	Description	Units
N	Number of loops	-
T, T^{in}	Outlet and inlet temp. of the field	ºC
T_j, T_j^{in}	Outlet and inlet temp. of loop j	ºC
$\bar{T}$	Mean inlet-outlet temperature	ºC
T^a	Ambient temperature	ºC
q^{T}	Total HTF flow in the field	l/s
q_j	HTF rate in loop j	l/s
ρ_f	Density of the HTF	kg/m^3
c_f	Specific heat capacity of the HTF	J/(kg ºC)
I	Direct solar irradiance	W/m^2
H_j	Thermal losses coef. of loop j	W/(m^2 ºC)
L	Loop length	m
S	Reflective surface of each loop	m^2
a_f	Cross-sectional area of the fluid	m^2
η	Efficiency of the collectors	-
α_j, β_j	Cleanliness and loss scale factor of j	-

2.2 System characteristics and constraints

Let the inlet temperature of each loop be equal to the inlet temperature of the field, that is, $T_j^{in} = T^{in}$, $\forall j \in \mathcal{L}$. We consider the inlet and ambient temperatures of the field and the DNI as disturbances that can be measured or estimated. Moreover, the outlet temperature of the solar field can be calculated as

$$T = \frac{\sum_{j\in\mathcal{L}} T_j q_j}{q^{\mathrm{T}}}, \quad (3)$$

where the total HTF flow is computed as $q^{\mathrm{T}} = \sum_{j\in\mathcal{L}} q_j$.

In addition, we must consider constraints due to the minimum and maximum temperatures supported by the HTF (4a), restrictions in the flow rate of each loop due to the operating limits of the pump (4b), and an upper bound in the total flow rate in the field (4c):

$$T^{\min} \le T_j \le T^{\max},\ \ \forall j \in \mathcal{L}, \quad (4a)$$

$$q^{\min} \le q_j \le q^{\max},\ \ \forall j \in \mathcal{L}, \quad (4b)$$

$$q^{\mathrm{T}} \le q^{\mathrm{T,max}}. \quad (4c)$$

Note that although the dynamics of the different loops are independent, they are coupled by the constraint (4c).

Remark 1. According to the values of the operational constraints for the ACUREX solar field in Camacho et al. (2012), the inequality $Nq^{\min} \le q^{\mathrm{T,max}} \le Nq^{\max}$ holds.

2.3 Linear discrete-time model of the system

The main objective of the control system is to keep the outlet temperature and the HTF flow of the field close to a given set point despite disturbances. To do so, we linearize the lumped model of each loop (2) around a desired operating point $\left(T_j^\circ, q_j^\circ\right)$, and redefine the local variables of each loop (T_j, q_j) as the sum of their value at the operating point plus a small signal variable (x_j, u_j):

$$T_j = T_j^\circ + x_j,\ q_j = q_j^\circ + u_j,\ \ \forall j \in \mathcal{L}. \quad (5)$$

Assumption 1. Since we study small variations around the operating point, we suppose that the temperature-dependent parameters are fixed at a temperature value equal to T_j° and therefore are assumed to be constant. We identify them in the linear model with the superscript $^\circ$.

Considering (2) and (5), we obtain the linearized lumped model for each loop $j \in \mathcal{L}$:

$$C_j^\circ \frac{dx_j}{dt} = -\left(P_j^\circ q_j^\circ + \frac{\beta_j SH_j^\circ}{2}\right) x_j - P_j^\circ \left(T_j^\circ - T^{in}\right) u_j + \alpha_j \eta SI - q_j^\circ P_j^\circ \left(T_j^\circ - T^{in}\right) - \frac{\beta_j SH_j^\circ}{2}\left(T_j^\circ + T^{in} - 2T^a\right). \tag{6}$$

Using the forward Euler method and grouping terms in (6), we can express the model of each loop as

$$x_j(k+1) = A_j x_j(k) + B_j u_j(k) + w_j(k), \quad \forall j \in \mathcal{L}. \tag{7}$$

By aggregating (7) for all loops $j \in \mathcal{L}$, we can describe the model of the whole field as

$$x(k+1) = Ax(k) + Bu(k) + w(k), \tag{8}$$

where $x(k) = [x_j(k)]_{j\in\mathcal{L}} \in \mathbb{R}^N$, $u(k) = [u_j(k)]_{j\in\mathcal{L}} \in \mathbb{R}^N$, $w(k) = [w_j(k)]_{j\in\mathcal{L}} \in \mathbb{R}^N$, $A = \mathrm{diag}(A_j)_{j\in\mathcal{L}} \in \mathbb{R}^{N\times N}$, and $B = \mathrm{diag}(B_j)_{j\in\mathcal{L}} \in \mathbb{R}^{N\times N}$.

Additionally, constraints (4) can be rewritten in terms of the deviation variables (5) as

$$T^{\min} - T_j^\circ \le x_j(k) \le T^{\max} - T_j^\circ, \quad \forall j \in \mathcal{L} \tag{9a}$$

$$q^{\min} - q_j^\circ \le u_j(k) \le q^{\max} - q_j^\circ, \quad \forall j \in \mathcal{L} \tag{9b}$$

$$\sum_{j\in\mathcal{L}} u_j(k) \le q^{\mathrm{T,max}} - \sum_{j\in\mathcal{L}} q_j^\circ. \tag{9c}$$

3. CONTROL STRATEGY

Since we cannot manipulate the energy received by the collectors, we use the HTF flow as a control input for our system. As mentioned in Section 2.3, the main control goal is to regulate variables (x_j, u_j) towards the origin, so that the system is kept close to the desired operating point (T_j°, q_j°), for all $j \in \mathcal{L}$. In particular, the centralized MPC problem is defined as follows

$$\begin{aligned} \min_{\mathbf{u}(k)} \sum_{n=0}^{N_\mathrm{p}-1} \Big(& x(k+n+1)^\top Q x(k+n+1) \\ & + u(k+n)^\top R u(k+n) \Big), \\ \text{s.t. } & (8) \text{ and } (9), \end{aligned} \tag{10}$$

where n denotes the time step along the prediction horizon N_p, and the weighting matrices Q and R are positive definite. Let us describe the vector $\mathbf{u}(k)$ as the sequence of inputs $\mathbf{u}(k) = \left[u(k)^\top, u(k+1)^\top, \ldots, u(k+N_\mathrm{p}-1)^\top\right]^\top$.

Addressing (10) through standard centralized MPC approaches for a large-scale system such as the solar plant can lead to an unfeasible application for real-time control. For this reason, this paper proposes a coalitional MPC approach that divides the global problem into several subproblems that can be solved in a decentralized manner by a set of local controllers. In this way, we can solve several independent problems in parallel that would lead to lower computational costs.

According to Remark 1, if we want to solve Problem (10) in a decentralized manner, we need a resource allocation mechanism to distribute the total flow constraint. All loops cannot be saturated at the same time at their maximum local value $q^{\max}$ because (4c) would not be satisfied.

3.1 Coalitional control architecture

We will proceed as in previous coalitional approaches applied to solar fields, such as that of Masero et al. (2022), where the parabolic-trough plant is considered a cooperative network, described by a graph $\mathcal{G}(k) = (\mathcal{L}, \mathcal{E}(k))$. The set of loops is denoted as $\mathcal{L}$, and we assume that each loop $j \in \mathcal{L}$ is managed by a local controller or agent. Moreover, loops will be interconnected by a set of links $\mathcal{E}(k)$, with $\mathcal{E}(k) \subseteq \mathcal{L} \times \mathcal{L}$. The state of these links is dynamically switched between enabled and disabled according to the system requirements. When a given link is enabled, agents of the corresponding connected loops can share data through a bidirectional information flow.

At time instant k, the graph $\mathcal{G}(k)$ defines the partition of the system $\mathcal{P}(k) = \{\mathcal{C}_1, \mathcal{C}_2, \ldots, \mathcal{C}_{|\mathcal{P}(k)|}\}$ as the set of $|\mathcal{P}(k)|$ non-empty clusters or coalitions of loops, which satisfy $\mathcal{C}_i \cap \mathcal{C}_\ell = \emptyset$ for any $i \neq \ell$. Agents within a coalition $\mathcal{C}_i$ operate as a single controller or entity. The size of $\mathcal{C}_i$ can range from a single loop $\mathcal{C}_i = \{j\}$, i.e., $|\mathcal{C}_i| = 1$, to the grand coalition $\mathcal{C}_i = \mathcal{L}$, i.e., $|\mathcal{C}_i| = N$.

Remark 2. The partition $\mathcal{P}(k)$ of the field can be computed following different criteria such as associating loops that are geographically close, grouping loops with different flow requirements, or clustering loops that receive higher solar irradiance with those that are shaded or less efficient. From now on, we will refer to the last criteria as grouping *unbalanced* loops in terms of effective DNI.

3.2 Decentralized control goal

Let us define $q_{\mathcal{C}_i}^{\max}(k)$ as a virtual state that models a *pool* of the flow available for a given coalition $\mathcal{C}_i \in \mathcal{P}(k)$. Consequently, the loops within a coalition will need to satisfy $\sum_{j\in\mathcal{C}_i} q_j(k) \le q_{\mathcal{C}_i}^{\max}(k)$, since $q_{\mathcal{C}_i}^{\max}(k)$ represents the maximum flow constraint for every coalition. In terms of deviation or small signal variables, we can rewrite the previous expression as

$$\sum_{j\in\mathcal{C}_i} u_j(k) \le q_{\mathcal{C}_i}^{\max}(k) - \sum_{j\in\mathcal{C}_i} q_j^\circ. \tag{11}$$

To fulfill the maximum flow constraint (4c) in a decentralized manner, we start by distributing $q^{\mathrm{T,max}}$ proportionally between the different coalitions that form the partition

$$q_{\mathcal{C}_i}^{\max}(0) = \frac{|\mathcal{C}_i| q^{\mathrm{T,max}}}{|\mathcal{L}|}, \quad \forall \mathcal{C}_i \in \mathcal{P}(k). \tag{12}$$

We will enhance the state of each coalition $x_{\mathcal{C}_i}$ to include the aforementioned virtual state $q_{\mathcal{C}_i}^{\max}$ so that we can optimize the maximum flow constraint for a given coalition:

$$x_{\mathcal{C}_i}(\cdot) = \left[\{x_j(\cdot)^\top\}_{j\in\mathcal{C}_i}, \ q_{\mathcal{C}_i}^{\max}(\cdot)^\top\right]^\top, \tag{13}$$

with

$$q_{\mathcal{C}_i}^{\max}(k+1) = q_{\mathcal{C}_i}^{\max}(k) - s_{\mathcal{C}_i}(k). \tag{14}$$

The new control variable $s_{\mathcal{C}_i}(k)$ corresponds to the amount of flow that a coalition does not need to satisfy its control goal, which can be transferred to other coalitions. As a result, we enlarge the input vector of a coalition $u_{\mathcal{C}_i}$ as

$$u_{\mathcal{C}_i}(\cdot) = \left[\{u_j(\cdot)^\top\}_{j\in\mathcal{C}_i}, \ s_{\mathcal{C}_i}(\cdot)^\top\right]^\top. \tag{15}$$

Moreover, $s_{\mathcal{C}_i}(k)$ must meet the following requirement:

$$0 \leq s_{\mathcal{C}_i}(k) \leq \sum_{j \in \mathcal{C}_i} q_j(k). \tag{16}$$

That is, $s_{\mathcal{C}_i}(k)$ must be positive because coalitions cannot take flow from other coalitions; they can only transfer their excess. Also, coalitions cannot share flow beyond the needs of the loops $j \in \mathcal{C}_i$. Consequently, flow sharing between coalitions is allowed, as there may be coalitions that require more HTF to regulate their loops, while others may have an excess that can be ceded. In particular, we define the subset $\mathcal{D}(k) \subseteq \mathcal{P}(k)$ as the coalitions $\mathcal{C}_i$ that require flow, satisfying $s_{\mathcal{C}_i}(k) = 0$. On the other hand, the subset $\mathcal{S}(k) \subseteq \mathcal{P}(k)$ contains coalitions $\mathcal{C}_i$ that satisfy $s_{\mathcal{C}_i}(k) > 0$, and therefore have an excess flow available to share. Note that $\mathcal{D}(k) \cap \mathcal{S}(k) = \emptyset$ and $\mathcal{D}(k) \cup \mathcal{S}(k) = \mathcal{P}(k)$. Let us also define $s_{\mathrm{T}}(k) \triangleq \sum_{\mathcal{C}_i \in \mathcal{P}(k)} s_{\mathcal{C}_i}$ as the total excess at time instant k. Note that, as $s_{\mathcal{C}_i}(k) = 0$ for $\mathcal{C}_i \in \mathcal{D}(k)$, it is not relevant if $s_{\mathrm{T}}(k)$ is calculated as the sum of the excess of partition $\mathcal{P}(k)$ or of the subset $\mathcal{S}(k)$.

The local control objective for every coalition $\mathcal{C}_i \in \mathcal{P}(k)$ is given by

$$\begin{aligned} \min_{\mathbf{u}_{\mathcal{C}_i}(k)} \; & \sum_{n=0}^{N_{\mathrm{p}}-1} \Big(x_{\mathcal{C}_i}(k+n+1) Q_{\mathcal{C}} x_{\mathcal{C}_i}(k+n+1) \\ & \qquad + u_{\mathcal{C}_i}(k+n) R_{\mathcal{C}} u_{\mathcal{C}_i}(k+n) \Big) \\ \text{s.t. } & (7), (9a), (9b), \; \forall j \in \mathcal{C}_i, \\ & (11), (14), (16), \end{aligned} \tag{17}$$

where $Q_{\mathcal{C}}$ and $R_{\mathcal{C}}$ are positive definite weighting matrices, and $\mathbf{u}_{\mathcal{C}_i}(k) = \left[u_{\mathcal{C}_i}(k)^\top, \ldots, u_{\mathcal{C}_i}(k+N_{\mathrm{p}}-1)^\top\right]^\top$, with vector $u_{\mathcal{C}_i}(\cdot)$ defined in (15).

3.3 Control scheme

Loops within coalitions $\mathcal{C}_i \in \mathcal{D}(k)$ cannot reach their operating point with the flow they have available and request flow. On the contrary, coalitions $\mathcal{C}_i \in \mathcal{S}(k)$ have a surplus and will make their flow excess available to the rest. This allows us to create an event-based flow-sharing mechanism that, between coalitions, distributes the flow constraint dynamically.

We are dealing with a resource allocation problem in which the shared resource is the maximum value of the flow rate in the whole field $q^{\mathrm{T,max}}$. The flow-sharing mechanism between coalitions described in Section 3.2 will allow the initial value of $q^{\max}_{\mathcal{C}_i}$ (see (12)) to change according to the needs of the loops belonging to $\mathcal{C}_i$. By means of dynamic sharing of the flow constraint, we fulfill the coupled constraint (4c), as $\sum_{\mathcal{C}_i \in \mathcal{P}(k)} q^{\max}_{\mathcal{C}_i}(k) = q^{\mathrm{T,max}}$, for every time instant k. To address this problem, we propose a two-layer coalitional MPC for constrained coupled subsystems. The control scheme has been summarized in Algorithm 1.

Algorithm 1 Overall control scheme.

Initialization. At $k = 0$, we distribute $q^{\mathrm{T,max}}$ as in (12). At each time instant k:

Top layer:

1. The field partition $\mathcal{P}(k)$ is computed by grouping unbalanced loops regarding the effective solar irradiance they receive. To this end, we define a vector $\mathbf{I}_k$ that sorts the effective solar irradiance received by loops $j \in \mathcal{L}$ at time instant k in a descending order. Coalitions are made by grouping the loops at the beginning of the vector $\mathbf{I}_k$ with those at the end.
2. If $\mathcal{D}(k) \neq \emptyset$ and $\mathcal{S}(k) \neq \emptyset$, the excess $s_{\mathrm{T}}(k)$ is distributed among coalitions $\mathcal{C}_i \in \mathcal{D}(k)$ following $q^{\max}_{\mathcal{C}_i}(k+1) = q^{\max}_{\mathcal{C}_i}(k) + \Delta_{\mathcal{C}_i}(k)$, where
$$\Delta_{\mathcal{C}_i}(k) = \frac{|\mathcal{C}_i| s_{\mathrm{T}}(k)}{|\mathcal{L}_{\mathcal{D}(k)}|}, \;\; \forall \mathcal{C}_i \in \mathcal{D}(k), \tag{18}$$
with $|\mathcal{L}_{\mathcal{D}(k)}|$ being the total number of loops in the subset $\mathcal{D}(k)$. On the other hand, the maximum flow constraint for $\mathcal{C}_i \in \mathcal{S}(k)$ is updated as (14).
3. If $\mathcal{D}(k) = \emptyset$, then $\mathcal{S}(k) = \mathcal{P}(k)$. In this case, the total excess $s_{\mathrm{T}}(k)$ is proportionally distributed among all coalitions using
$$\Delta_{\mathcal{C}_i}(k) = \frac{|\mathcal{C}_i| s_{\mathrm{T}}(k)}{|\mathcal{L}|}, \;\; \forall \mathcal{C}_i \in \mathcal{P}(k). \tag{19}$$
The maximum flow constraint for all $\mathcal{C}_i \in \mathcal{P}(k)$ is updated as $q^{\max}_{\mathcal{C}_i}(k+1) = q^{\max}_{\mathcal{C}_i}(k) - s_{\mathcal{C}_i}(k) + \Delta_{\mathcal{C}_i}(k)$.

Bottom layer:

3. For every coalition $\mathcal{C}_i \in \mathcal{P}(k)$, the local optimization problem (17) is solved subject to the most recent maximum flow constraint provided by the top layer as a consequence of the flow-sharing between coalitions.
4. According to (15) and the optimal sequence $\mathbf{u}_{\mathcal{C}_i}(k)$, loops $j \in \mathcal{C}_i$ will apply to the first component of their input vectors $u_j(k)$, for all $\mathcal{C}_i \in \mathcal{P}(k)$.
5. For every coalition $\mathcal{C}_i \in \mathcal{P}(k)$ the first component of $s_{\mathcal{C}_i}(k)$ will determine:
   a) If $s_{\mathcal{C}_i}(k) = 0$, the coalition will send a flow request: $\mathcal{C}_i \in \mathcal{D}(k)$.
   b) If $s_{\mathcal{C}_i}(k) > 0$, the coalition has an excess flow which can make available: $\mathcal{C}_i \in \mathcal{S}(k)$.

4. SIMULATION RESULTS

In this section, we apply the proposed coalitional scheme on a parabolic-trough solar collector field such as the one described in Section 2, with $N = 100$ loops. The main objective is to control the plant around an operating temperature of 250°C, meeting the constraints described in the previous sections despite external disturbances. The 100-loop benchmark has been simulated using an hour and a half DNI profile to model the solar radiation, setting the radiation to zero in the passive segments of the loops, corresponding to the sections $\{37-42\}$, $\{79-96\}$, and $\{133-138\}$, of the $L = 174$ m loop. For simplicity, we consider the ambient temperature T^a of the field and the inlet temperature T^{in} of the HTF as constant parameters along the simulation length $t_{\mathrm{T}} = 90$min.

The results obtained using the coalitional approach of Algorithm 1 will be compared with those obtained with

I. Centralized MPC, which solves Problem (10).
II. Decentralized MPC, where each loop $j \in \mathcal{L}$ is governed by a local controller with no information from the rest that solves

$$\begin{aligned} \min_{\mathbf{u}_j(k)} \; & \sum_{n=0}^{N_{\mathrm{p}}-1} \Big(x_j(k+n+1)^\top Q_j x_j(k+n+1) \\ & \qquad + u_j(k+n)^\top R_j u_j(k+n) \Big), \\ \text{s.t. } & (7), (9a), (9b), \\ & u_j(k) \leq q^{\max}_{\mathcal{C}_i}(0) - q^{\circ}_j, \end{aligned} \tag{20}$$

where Q_j and R_j are set according to the global matrices in (10), and $\mathbf{u}_j(k)$ is defined as the sequence of inputs $u_j(\cdot)$ from $n = k$ to $k + N_\mathrm{p} - 1$.

Remark 3. Problem (20) is solved without the resource-sharing mechanism between loops proposed in Algorithm 1. Therefore, the maximum flow constraint is simply set according to (12) with $|\mathcal{C}_i| = 1$ for all $\mathcal{C}_i \in \mathcal{P}(k)$.

Let $\mathbf{P} = \sum_{k=1}^{t_\mathrm{T}} \sum_{j\in\mathcal{L}} \|u_j(k)\|_{R_j} + \|x_j(k+1)\|_{Q_j}$ be the index that will be used to evaluate the performance of a given control strategy during the simulation length t_T. In addition, we provide an average value for the computation time $\bar{\tau}$, which has been calculated as

$$\bar{\tau} = \frac{\sum_{k=1}^{t_\mathrm{T}} \tau(k)}{t_\mathrm{T}}, \quad \text{with} \quad \tau(k) = \frac{\sum_{\mathcal{C}_i\in\mathcal{P}} \tau_{\mathcal{C}_i}(k)}{|\mathcal{P}(k)|}, \qquad (21)$$

where $\tau(k)$ corresponds to the average computation time per coalition at the time instant k, and $\tau_{\mathcal{C}_i}(k)$ represents the time it takes a given coalition to solve its optimization problem. For the centralized MPC, we work with the grand coalition $\mathcal{C}_i = \mathcal{L}$, i.e., $|\mathcal{P}(k)| = 1$, and for the decentralized MPC we study $|\mathcal{P}(k)| = N$ singletons. Finally, we consider the parameters $S = 267.4$ m^2, $a_f = 7.55 \cdot 10^{-4}$ m^2, $\eta = 0.64$. The values of $\alpha_j \in [0.6, 1]$ and $\beta_j \in [1, 1.25]$ have been generated following a uniform random distribution. Also, the operational constraints have been set as $T^{\min} = 220$°C, $T^{\max} = 300$°C, $q^{\min} = 0.2$ l/s and $q^{\min} = 1.5$ l/s.

We have simulated the proposed coalitional algorithm for two different coalition sizes: $|\mathcal{C}_i| = 2$ and $|\mathcal{C}_i| = 10$. We study the behavior of the field when two moving clouds shade the collectors: a large cloud moves through the plant during $t = \{4 - 52\}$ min, while a smaller cloud crosses the field diagonally between $t = \{16 - 46\}$ min. The top layer of Algorithm 1 calculates the partition $\mathcal{P}(k)$ by clustering loops that receive more DNI with other loops that are less efficient or shaded by a cloud, according to Step 1 of Algorithm 1. A shaded loop will receive lower DNI, becoming less efficient, so that it can provide its remaining flow to other loops in the same coalition to increase their performance. In this sense, Fig. 1 shows the evolution of the field partition $\mathcal{P}(k)$ during the whole simulation when using $|\mathcal{C}_i| = 10$, where we can see the formation of new coalitions when the plant is affected by passing clouds. Loops represented with the same color at a given time instant belong to the same coalition.

Fig. 2 shows the evolution of the outlet temperature and HTF flow of 10 random loops of the 100-loop field. As mentioned in Section 2.1, the scale factors α_j and β_j will model the cleanliness and thermal losses of each loop, respectively. A small value of α_j represents loops with dirtier collectors and therefore will receive less effective solar irradiance. In turn, a high value of β_j represents loops with greater thermal losses. Both of these characteristics make loops less efficient, stabilizing at low flow value q_j°. See, for example, the differences in the evolution of loop #5 (red line) and #35 (yellow line) in Fig. 2. Loop #35 stabilizes at a high flow value at its operating point, and the passing clouds practically do not affect its outlet temperature. Therefore, loop #35 is more efficient than #5, since the effect of the clouds in the latter is much more notable. Loops tend to decrease their flow value $q_j(t)$ when a cloud shades them. In this regard, efficient

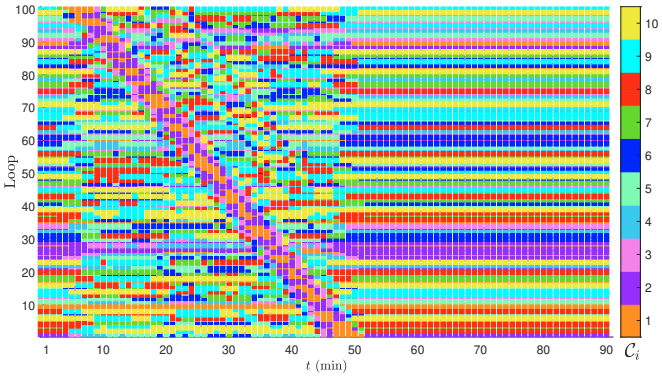

Fig. 1. Coalition forming when using $|\mathcal{C}_i| = 10$.

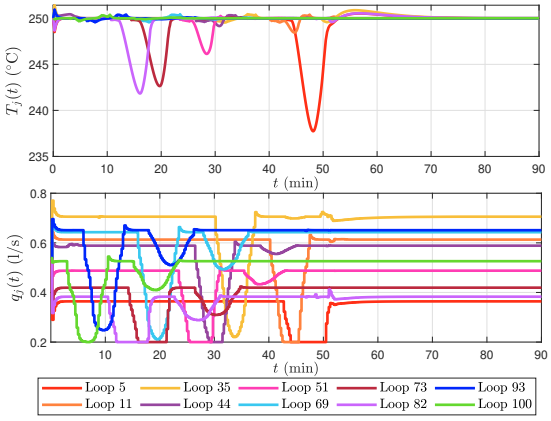

Fig. 2. Outlet temperature and HTF flow for 10 random loops when using the $|\mathcal{C}_i| = 10$ coalitional approach.

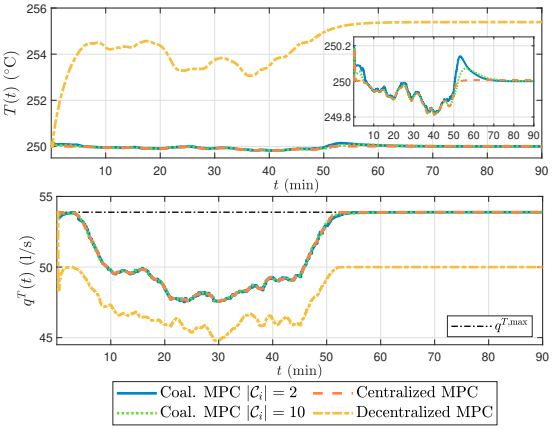

Fig. 3. Outlet temperature and total HTF flow of the 100-loop field using different control strategies.

loops that stabilize at a higher HTF flow value will have more margin to decrease their local flow when a cloud affects them, maintaining the outlet temperature in its operating value. For example, loop #93 (dark-blue line) manages to maintain its outlet temperature around 250°C by decreasing its flow value. On the other hand, less efficient loops, such as #82 (light-purple line), drop the value of its flow but saturates at its lower bound $q^{\min}$.

Fig. 3 compares the evolution of the outlet temperature and the total flow of the field when using different control strategies. Blue solid lines represent the result using the coalition algorithm proposed with $|\mathcal{C}_i| = 2$, while the green dotted lines represent the evolution using $|\mathcal{C}_i| = 10$. The

orange dashed lines represent the centralized MPC result, and the yellow dashed-dotted lines show the evolution when a decentralized MPC is applied. In the bottom plot, the black dashed-dotted line represents the maximum flow allowed in the field, which is equal to the operating point. The presence of clouds directly affects the solar radiation received by the collector, which decreases significantly, reducing the field outlet temperature and HTF flow.

In the coalitional scheme, loops transfer and absorb flow according to the needs of the system, shrinking and enlarging their constraint set $q_{\mathcal{C}_i}^{\max}$. As can be seen in Fig. 3, the coalitional scheme takes longer to recover from the cloud event and regulate the value of the temperature, since conflicts with the shared resource appear when loops work close to the operating point. However, Algorithm 1 using $|\mathcal{C}_i| = 10$ and $|\mathcal{C}_i| = 2$ results in a decrease in the overall performance $\mathbf{P}$ of 0.82% and 3.6%, respectively, with respect to the centralized solution. Considering a smaller size of coalitions implies that we have more agents working in parallel, but at the same time, these local controllers handle less amount of information. In this regard, the centralized MPC results in an average time of $\bar{\tau} = 3.5998$ s, while the coalitional approach significantly reduces the computation time to $\bar{\tau} = 0.1998$ s with $|\mathcal{C}_i| = 2$, and $\bar{\tau} = 0.4553$ s with $|\mathcal{C}_i| = 10$. The centralized approach solves Problem (10) using a single controller, while in the coalitional approach, $|\mathcal{P}(k)|$ controllers work in parallel. Thus, considering larger coalitions results in a longer computational time, but also in better performance than when considering smaller coalitions.

Finally, applying a local MPC to each loop of the $N = 100$ plant is not feasible even if the computing time is minimal for each loop ($\bar{\tau} = 0.0363$ s). In this case, loops solve independent optimization problems (see Problem (20)) without information about other loops. For this reason, the maximum flow constraint of a given loop cannot change during the simulation. We are not allowing the loops to dynamically distribute their excess flow, nor are we allowing them to demand more, so there are loops that need to increase their flow and cannot. This, besides increasing the performance index $\mathbf{P}$ in a $9.1 \cdot 10^3\%$, may cause the violation of the operational constraints, in addition to not complying with the control objective.

5. CONCLUSIONS

We have presented a two-layer coalitional model predictive control approach for the regulation of a parabolic-trough solar collector field that allows us to distribute the large-scale optimization problem. We have dealt with constraint-coupled subsystems, and distributed the coupled constraint using a resource-sharing mechanism to solve the optimization in a decentralized manner while guaranteeing the satisfaction of operational constraints. Furthermore, simulation results demonstrate that we achieve a small performance loss with respect to the centralized solution, as well as reducing the computational load.

Further research should focus on applying this idea to the non-linear concentrated parameter model of the plant, adapting the control objective to maximize the thermal power. To exploit the algorithm's scalability, we should apply this methodology to larger solar fields, since coalitional approaches arise as a possible solution to the drawbacks that stem from the requirements of large-scale systems.

REFERENCES

Alsharkawi, A. and Rossiter, J. (2016). Dual mode mpc for a concentrated solar thermal power plant. In *Proceedings of the* 11^{th} *IFAC Symposium on Dynamics and Control of Process Systems, Including Biosystems*, volume 49, 260–265.

Baldivieso-Monasterios, P.R. and Trodden, P.A. (2021). Coalitional predictive control: Consensus-based coalition forming with robust regulation. *Automatica*, 125, 109380.

Barreiro-Gomez, J., Ocampo-Martinez, C., Maestre, J., and Quijano, N. (2015). Multi-objective model-free control based on population dynamics and cooperative games. In *2015 54th IEEE Conference on Decision and Control (CDC)*, 5296–5301.

Camacho, E.F., Berenguel, M., and Rubio, F.R. (1997). *Advanced Control of Solar Plants*. Springer London, London.

Camacho, E.F., Berenguel, M., Rubio, F.R., and Martínez, D. (2012). *Control of Solar Energy Systems*. Springer London, London.

Camacho, E., Rubio, F., Berenguel, M., and Valenzuela, L. (2007). A survey on control schemes for distributed solar collector fields. part i: Modeling and basic control approaches. *Solar Energy*, 81(10), 1240–1251.

Carmona, R. (1985). *Modeling and control of a distributed solar collector field with a one-axis tracking system.* Ph.D. thesis, University of Seville, Spain. (in Spanish).

Fele, F., Maestre, J.M., and Camacho, E.F. (2017). Coalitional control: Cooperative game theory and control. *IEEE Control Systems*, 37(1), 53–69.

Islam, M.T., Huda, N., Abdullah, A., and Saidur, R. (2018). A comprehensive review of state-of-the-art concentrating solar power (csp) technologies: Current status and research trends. *Renewable and Sustainable Energy Reviews*, 91, 987–1018.

Kabir, E., Kumar, P., Kumar, S., Adelodun, A.A., and Kim, K.H. (2018). Solar energy: Potential and future prospects. *Renewable and Sustainable Energy Reviews*, 82, 894–900.

La Bella, A., Klaus, P., Ferrari-Trecate, G., and Scattolini, R. (2021). Supervised model predictive control of large-scale electricity networks via clustering methods. *Optimal Control Applications and Methods*, 43, 44–64.

Masero, E., Maestre, J.M., and Camacho, E.F. (2022). Market-based clustering of model predictive controllers for maximizing collected energy by parabolic-trough solar collector fields. *Applied Energy*, 306, 117936.

Rathore, N., Panwar, N.L., Yettou, F., and Gama, A. (2021). A comprehensive review of different types of solar photovoltaic cells and their applications. *International Journal of Ambient Energy*, 42(10), 1200–1217.

Vasallo, M.J. and Bravo, J.M. (2016). A MPC approach for optimal generation scheduling in CSP plants. *Applied Energy*, 165(C), 357–370.

Zhang, H., Baeyens, J., Degrève, J., and Cacères, G. (2013). Concentrated solar power plants: Review and design methodology. *Renewable and Sustainable Energy Reviews*, 22, 466–481.